Electronic Supplementary Material (ESI) for Chemical Communications

Supporting Information

Stable Cu Nanoclusters: From Aggregation-Induced Emission Mechanism to Biosensing and Catalytic Applications

Xiaofang Jia,[a,b] Xuan Yang,[a,b] Jing Li,[a] Dongyue Li[a,b] and Erkang Wang*[a]

[a] *State Key Laboratory of Electroanalytical Chemistry, Changchun Institute of Applied Chemistry, Chinese Academy of Sciences, Changchun, Jilin, 130022, China. E-mail: ekwang@ciac.jl.cn*

[b] *Graduate School of the Chinese Academy of Sciences, Beijing, 100039, China*

Corresponding author: Prof. Erkang Wang, Email: ekwang@ciac.jl.cn

EXPERIMENTAL SECTION

Chemicals and materials. D-penicillamine (DPA) and racemic DL-penicillamine (DLPA) were obtained from Alfa Aesar (Tianjin, China). Glucose oxidase (EC 1.1.3.4) was bought from Sigma-Aldrich. $Cu(NO_3)_2 \cdot 3H_2O$, $AgNO_3$, glucose, and other reagents were purchased from Beijing Chemical Works (Beijing, China). All reagents were of analytical reagent grade, and used as received. Water used throughout all experiments was purified with the Millipore system (18.2 MΩ). All glassware was washed with aqua regia and rinsed with ultrapure water.

Apparatus and characterization. A drop of clear CuNCs aqueous solution (pH 7.0) was carefully placed on the ultrathin pure carbon film and dried at ambient condition for transmission electron microscopy (TEM) characterization. TEM measurement was made on a JEM-2100F high-resolution transmission electron microscope (Netherlands) operated at 200 kV. A XL30 ESEM scanning electron microscope (SEM) was used to determine the morphology of the aggregates. The X-ray photoelectron spectroscopy (XPS) measurements were conducted using an ESCALAB-MKII 250 photoelectron spectrometer (VG Co.) with Al Kα X-ray radiation (1486.6 eV) for excitation. IR spectra were collected at wavenumbers ranging from 400 to 4000 cm^{-1} using a VERTEX Fourier transform infrared (FTIR) spectrometer (Bruker). Matrix-assisted laser-desorption ionization time of flight mass spectrometric (MALDI-TOF MS) studies were carried out using Bruker autoflex III smartbeam MALDI-TOF/TOF-MS (Germany). The spectra was collected in positive-ion mode using the matrix DCTB (*trans*-2-[3-(4-*tert*butylphenyl)-2-methyl-2-propenyldidene]malononitrile). Negative-ion electrospray ionization mass spectrometry (ESI MS) measurements were performed on a LTQ linear ion trap mass spectrometer (Thermo, San Jose, CA, USA), equipped with a conventional ESI source. UV-visible absorption spectra were taken on a Cary 50 Scan UV-visible spectrophotometer (Varian, USA). Fluorescence spectra were recorded on a Fluoromax-4 spectrofluorometer (Horiba Jobin Yvon Inc. France) using 2.5 nm/ 2.5 nm slit widths of excitation and emission. The photoluminescence quantum yield (QY) were measured directly with the absolute QY measurement system C9920-02

(Hamamatsu Photonics K. K., Japan), which comprises an excitation light source, monochromator, an integrating sphere capable of nitrogen gas flow and a CCD spectrometer for detecting the whole spectral range simultaneously. The luminescence decay curves were measured on a FLS920 spectrofluorometer (Edinburgh Instruments, UK) equipped with EPL375 pulsed laser diode (ns timescale), and a Lecroy Wave Runner 6100 Digital Osilloscope (1 GHz) using a tunable laser (pulse width = 4 ns, gate = 50 ns) as the excitation (Contimuum Sunlite OPO) (μs timescale).

Synthesis of CuNCs. In a typical systhesis, the DPA-mediated CuNCs were prepared by adding a 100 mM $Cu(NO_3)_2$ aqueous solution (40 μL) into a fresh aqueous solution (4 mL) containing 10 mM DPA in the vigorous stirring. After about 10 minutes, white precipitate was generated, displaying red luminescence under UV lamp irradiation. The mixture was stirred for 90 min under air at room temperature (20 °C). The precipitate was collected by centrifugation at 8000 rpm for 10 min followed by washing thoroughly with water for three times. Then the product was freeze-dried under the vacuum and stored in the refrigerator (-20 °C) for long-term preservation.

Synthesis of AgNCs. The DPA-protected AgNCs were synthesized in a similar method, except that the concentration of DPA was 4 mM.

Detection of H_2O_2 and glucose. A typical H_2O_2 detection procedure was conducted as follows. Different concentrations of H_2O_2 stock solutions (5 μL) were added to 1 mL as-prepared CuNCs, followed by incubation at room temperature for 4 hours. For the glucose detection, 5 μL of glucose solutions with different concentrations 37 °C for 30 min, 200 μL as-prepared CuNCs and 600 μL HAc-NaAc buffer (0.2 M, pH 4.0) were added for other 4 hours. To evaluate the selectivity of glucose fluorescence detection by using CuNCs, other carbohydrates were also tested and the response was recorded and analyzed.

Catalytic Reduction of MB Dye. The catalytic property of CuNCs was analyzed following the literature procedure.[1] In a typical procedure, different volumes of prepared CuNCs were added into 900

μL PB buffer (50 mM, pH 5.0) containing 33 μM MB dye and 60 mM N_2H_4. The blue color of the mixture faded quickly, indicating the catalytic reduction of the MB dye.

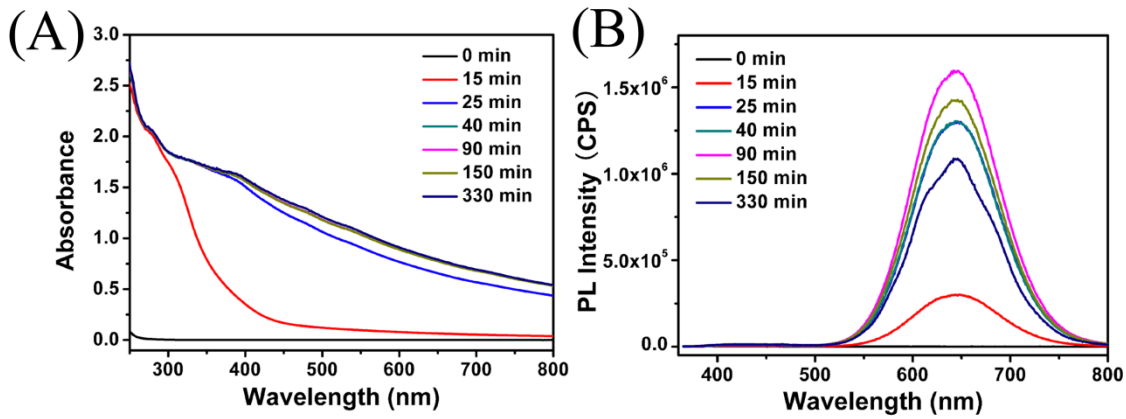

Fig. S1 Time-resolved evolution of (A) optical absorption and (B) PL spectra of CuNCs.

The absorption spectra of the forming CuNCs show absorption tails extending well into the long wavelength region. This implies that the large size of the CuNCs aggregates were formed in the aqueous solution, because it is well known that the Mie effect of nanoparticles causes such level-off tails in the absorption spectra. The level-off tails disappear after dissolving the aggregates by adjusting the pH (Fig. S8). As shown in Fig. S1B, the emission peak was somewhat distorted at 330 min. Under longer reaction time, strongly emissive CuNCs could be changed to no emissive or weakly emissive CuNCs, resulting in the decreased emission intensities.

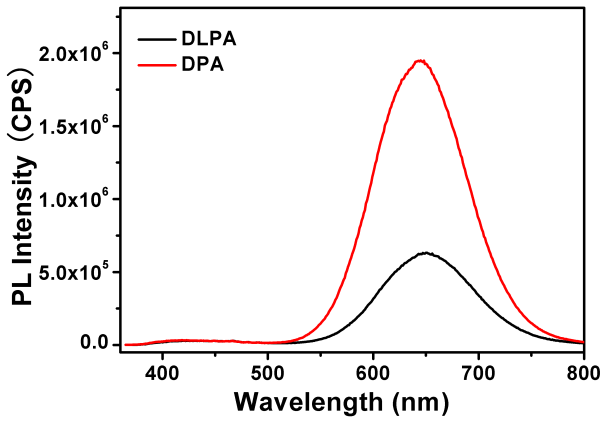

Fig. S2 PL spectra of chiral DPA-capped CuNCs and racemic DLPA-capped CuNCs.

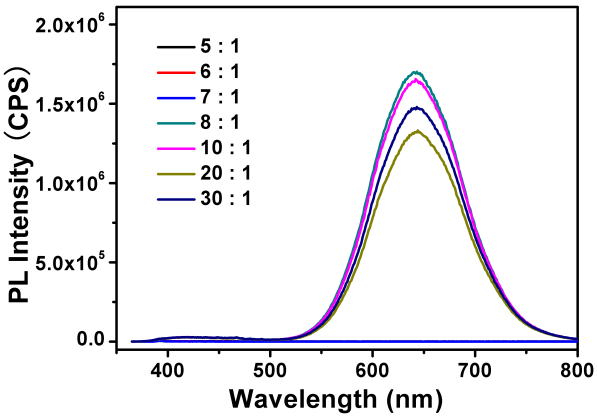

Fig. S3 PL spectra of CuNCs prepared with the different concentration ratio $R_{[DPA]/[Cu]}$ at a fixed Cu^{2+} concentration (1 mM).

Discussion of the formation of CuNCs.

To elucidate the reaction process fully, we present below our tentative suggestions for the formation of CuNCs. In our synthetic approach, DPA was found to be an effective ligand for both reduction and stabilization of CuNCs. Similar to the process of treating Wilson's disease,[2] the SH moiety plays a crucial role in the "reductive chelation" of the Cu^{2+} species *via* the reaction $2Cu^{2+} + 4RSH \rightarrow 2Cu^{+}\text{-}SR + RS\text{-}SR + 4H^{+}$ ($R = C_5H_9O_2N$). The reduction process is confirmed by the pH of reaction solution decreasing from 5.18 to 2.66 and the disappearance of the SH stretching band of free DPA at 2527 cm^{-1} (Fig. S6). On the basis of the pK_a values (pK_a=1.92 (COOH); 10.70 (NH_3^+)), the COOH groups are deprotonated to COO^- at pH 2.66, whereas NH_2 is protonated to NH_3^+, maximizing the zwitterionic electrostatic interactions. Then self-assembly of Cu^+-DPA into Cu^+-S(R)- repeat unit intermediate may occur, which attributes to the synergetic interplay of the electrostatic interaction among the R side chains and the $Cu^+\cdots Cu^+$ cuprophilic interaction.[3] The existence of excessive reductant DPA could facilitate Cu(I) aggregation to form CuNCs. It is worth mentioning that the chirality of DPA plays an important role for the creation of the brightly emissive CuNCs. In the control experiment, when racemic DLPA was adopted as ligand instead, the productive yield was only one-third of that of chiral DPA (Fig. S2). For the

racemic DLPA, the conformation is unfavorable for the electrostatic interaction between COO^- and NH_3^+, which would suppress the formation of particular aggregation of Cu^+-SR intermediate. Because clusters are less soluble in the lower pH and precipitate out of solution, the pH value plays a crucial role in the size-selecting progress by terminating or retarding the growth of clusters into larger ones; this provides an effective way of controlling cluster size.[4] On the other hand, at higher pH, for example, pH 7.5, no CuNCs were produced. At a fixed Cu^{2+} concentration (1 mM), the critical concentration ratio $R_{[DPA]/[Cu]}$ to form the CuNCs is as high as 8 (Fig. S3). The largely excessive DPA provides a reductive environment to prevent the oxidation of CuNCs upon exposure to air. This is consistent with our previous dsDNA protected CuNCs system, in which 10-fold ascorbic acid was needed.[5] Thus, the reaction conducted directly in the air condition instead of inert atmosphere, without the assistant of extra reducing agent, endowing the reaction with simplicity and good reproducibility.

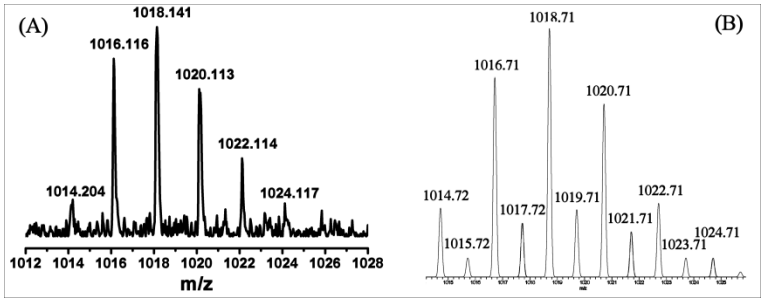

Fig. S4 (A) Experimental and (B) simulated isotopic pattern of $[Cu_6L_4\text{-}H+2Na]^+$.

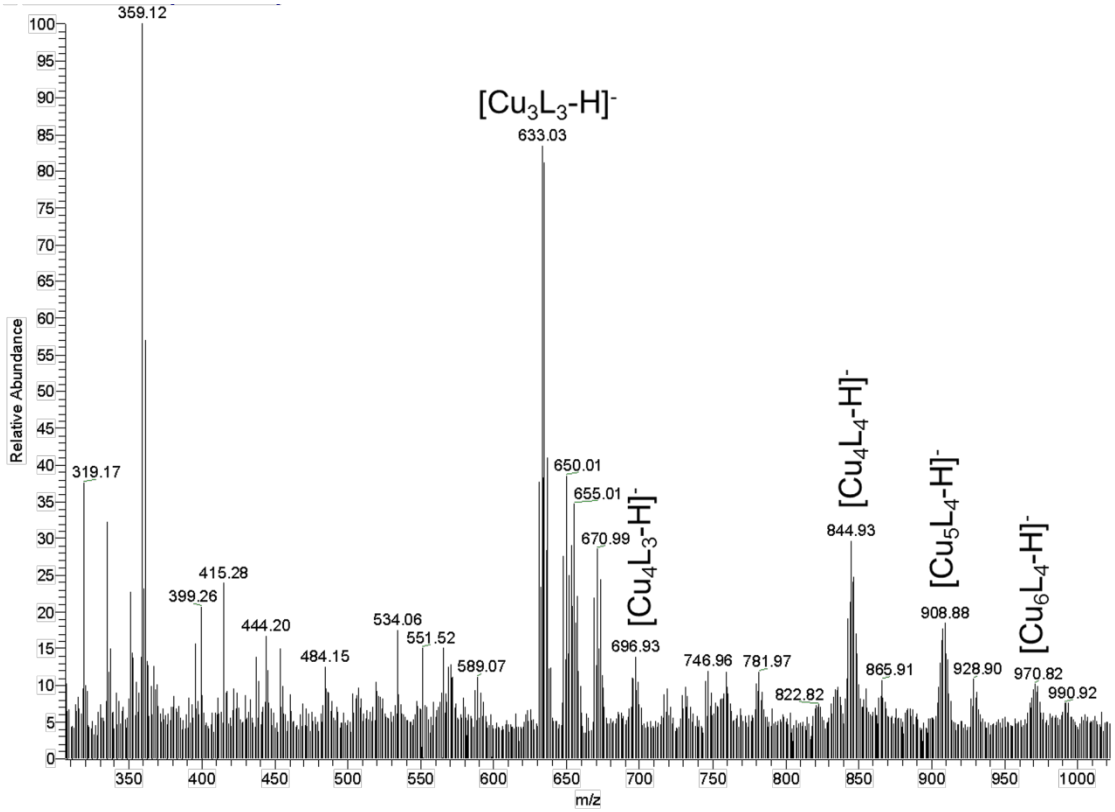

Fig. S5 Negative-ion ESI MS measurements of CuNCs (where L stands for $C_5H_{10}O_2NS$).

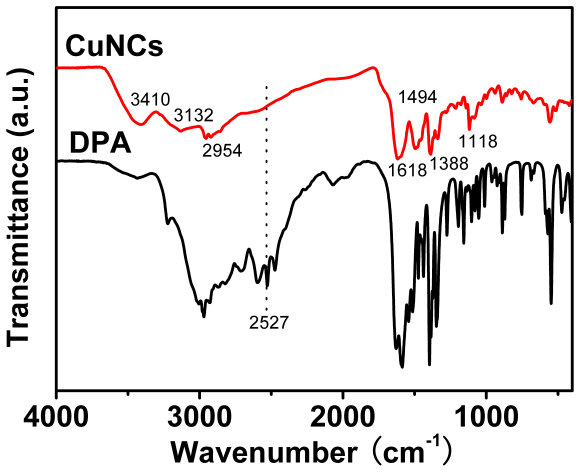

Fig. S6 FTIR spectra of pure DPA and DPA-capped CuNCs.

The surface-capping agents on CuNCs surfaces contain carboxylate (COO^-) and primary amino (NH_2) groups, which was confirmed by the presence of characteristic peaks for the stretch modes of COO^- (1388 and 1494 cm^{-1}) and those for the N-H stretch (3410 cm^{-1}) and the N-H bending (1618 cm^{-1}) of NH_2.

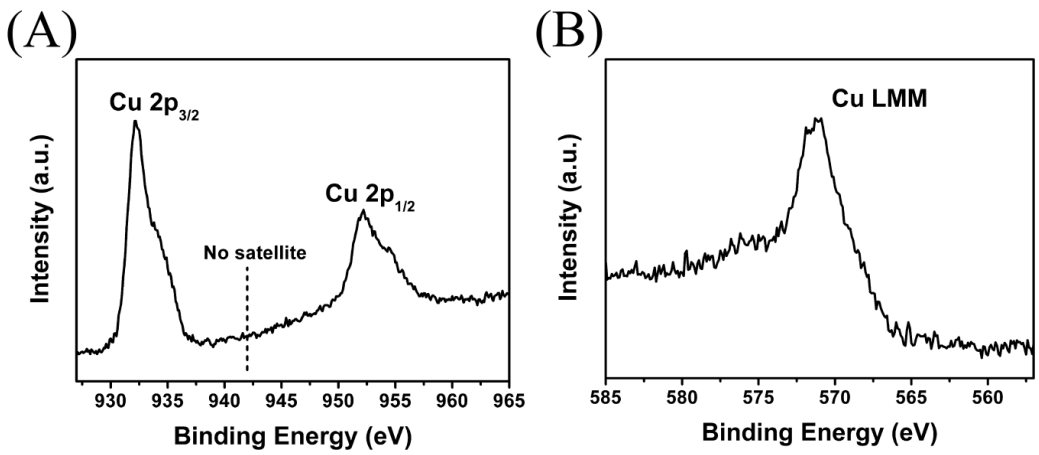

Fig. S7 (A) XPS of Cu 2p electrons and (B) the corresponding AES spectrum in the Cu LMM region of CuNCs.

The absence of Cu $2p_{3/2}$ satellite peak around 942 eV confirms that there is no existence of Cu^{2+}.[6] Two intense peaks at 952.7 and 933.0 eV are assigned to Cu $2p_{1/2}$ and $2p_{3/2}$, respectively. Due to the proximity of binding energy of Cu^0 and Cu^+, the oxidation state of Cu was further confirmed by AES. The AES Cu (LMM) peak at 570.9 eV indicates that the CuNCs are composed of Cu^+.[7]

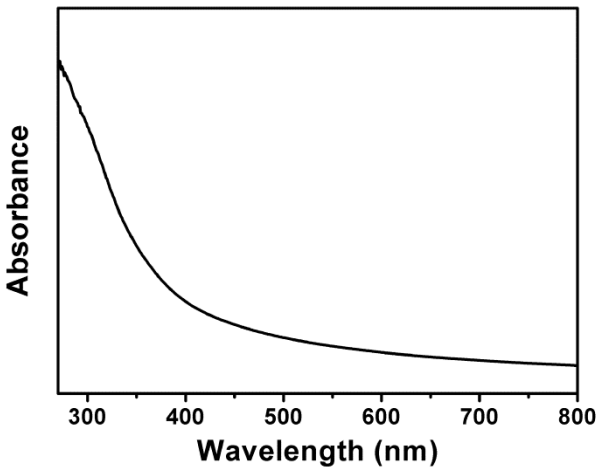

Fig. S8 Absorption spectra of the as-prepared CuNCs.

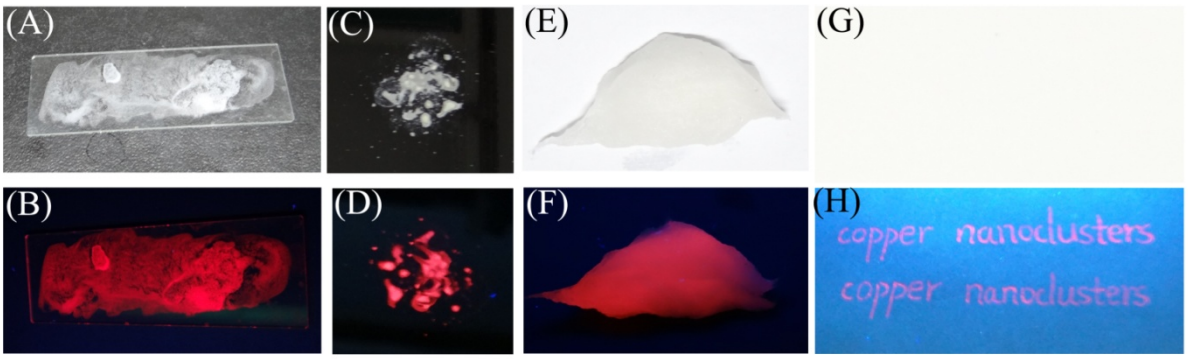

Fig. S9 Photographs of the CuNCs aqueous solution deposited on the surface of glass (A, B), silicon (C, D) and cotton (E, F) and commercially available paper (G, H) under the irradiation of daylight (top) and UV light (bottom); The words "copper nanoclusters" were written using CuNCs as ink in pen.

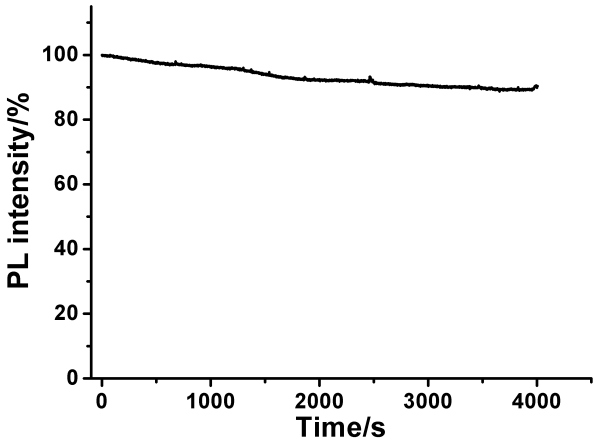

Fig. S10 The time-dependence of PL intensity at 640 nm emission (λ_{ex}=345 nm) of CuNCs in a fluorescence spectrophotometer. All the intensities are normalized according to the initial one.

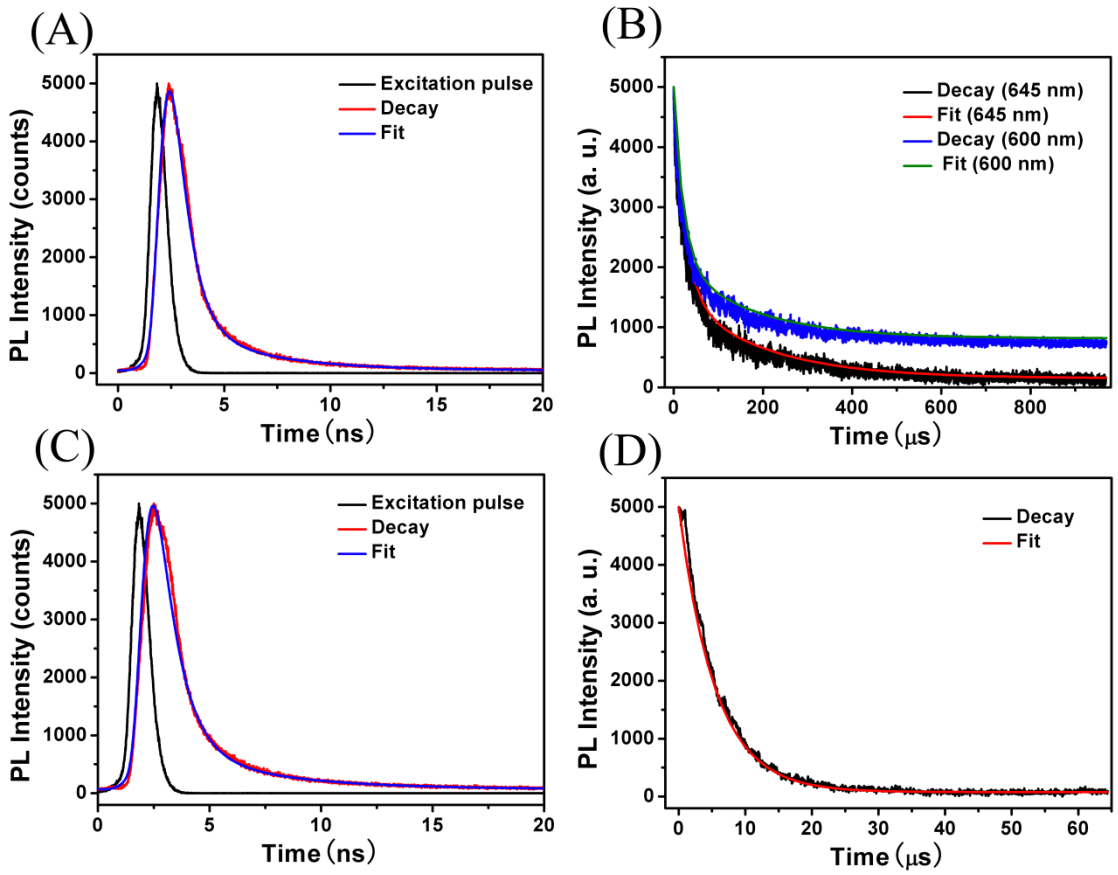

Fig. S11 PL decay profile (λ_{em} = 425 nm) of (A) CuNCs and (C) AgNCs at the excitation of 377 nm; PL decay profile of (B) CuNCs (λ_{em} = 600 nm and λ_{em} = 645 nm) and (D) AgNCs (λ_{em} = 588 nm) at the excitation of 355 nm. The fitted curves were overlaid on the experimental data.

Table S1 Lifetimes of DPA capped CuNCs and AgNCs at different emissions.

	CuNCs			AgNCs	
λ_{em} (nm)	425	600	645	425	588
λ_{ex} (nm)	377	355	355	377	355
τ□	0.75 ns	21.8 μs	24.6 μs	0.94 ns	5.44 μs
A_1 [a)]	66.3%	22.2%	23.4%	67.7%	100%
τ_2	3.80 ns	172.4 □μs	189.1 μs	4.45 ns	-
A_2	33.7%	77.8%	76.6%	32.3%	-
τ_{ave} [b)]	1.78 ns	139.0 μs	150.6 μs	2.07 ns	5.44 μs

a) The fractional contribution was calculated according to $A_i = \alpha_i\tau_i/\Sigma\alpha_j\tau_j$, where τ_i and α_i represent the decay time and the amplitudes of the components at t = 0, respectively; b) The average lifetime was calculated according to $\tau_{ave} = \Sigma A_i\tau_i$.

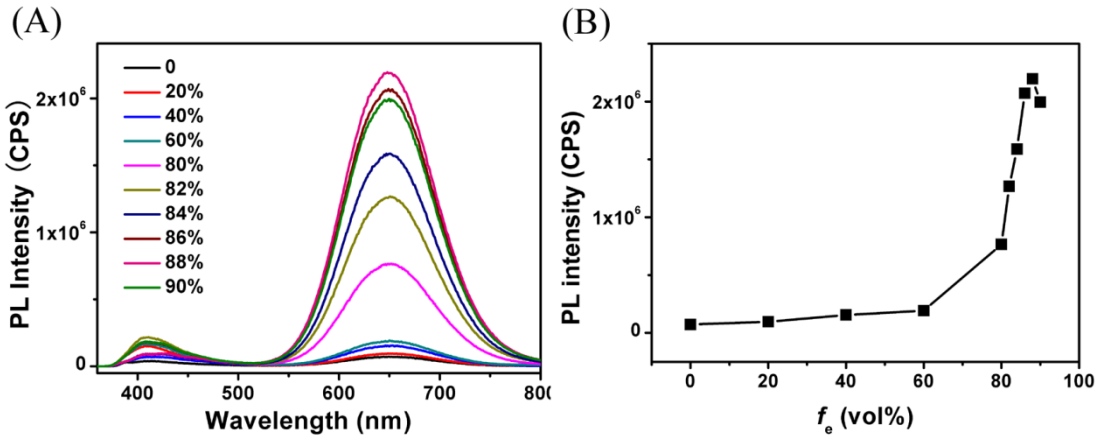

Fig. S12 (A) PL spectra of CuNCs solutions in ethanol-water mixtures with different volumetric fractions of ethanol (f_e, vol%). (B) Plots of PL intensity of CuNCs *versus* f_e.

To further confirm AIE property, CuNCs was dissolved in the aqueous solution (pH 7), and then different volumetric fractions of ethanol (bad solvent) was added. As shown in the Fig. S12, CuNC solutions in its good solvent are nearly non-emissive. Addition of large amounts of ethanol causes the CuNCs to aggregate and induces them to emit efficiently. In the solvent mixture with 88% ethanol, the PL intensity is 30-fold higher than that in the pure aqueous solution.

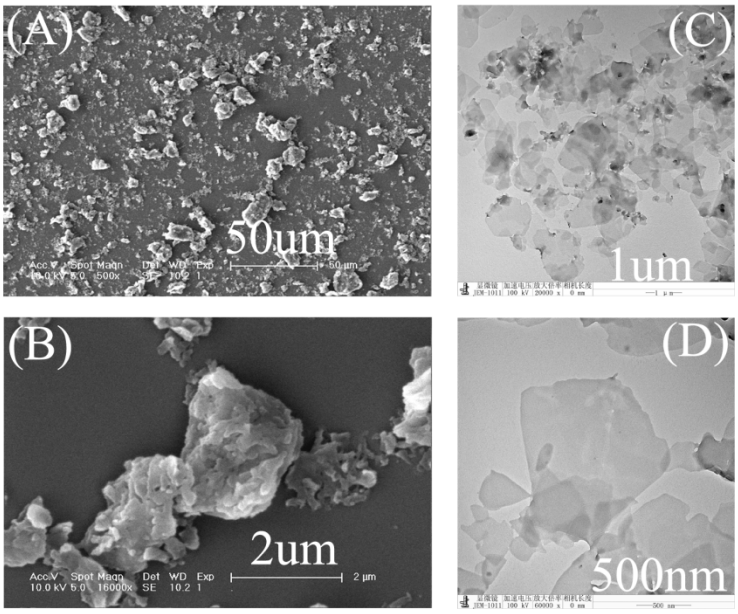

Fig. S13 SEM (A, B) and TEM (C, D) images of the CuNCs aggregates.

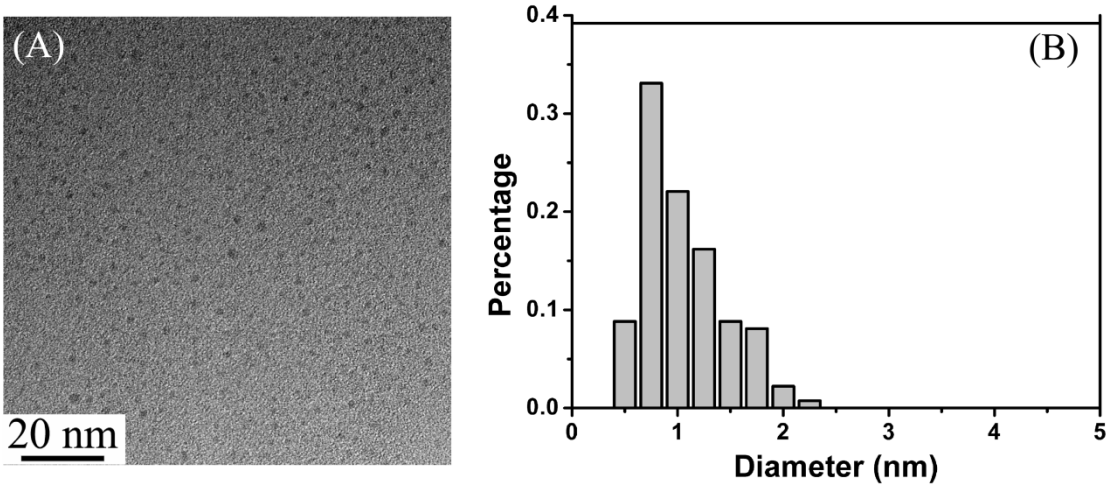

Fig. S14 (A)The representative HRTEM image and (B) size distribution of the as-prepared CuNCs in the dissolution state.

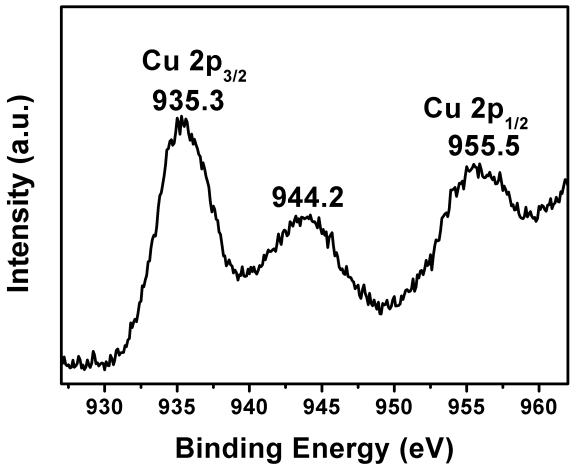

Fig. S15 XPS spectrum of Cu 2p electrons after CuNCs reacted with H_2O_2.

The peak corresponding to Cu $2p_{3/2}$ shifted to higher binding energy, accompanied by the appearance of a satellite peak at 944.2 eV, confirming that the Cu centers were oxidized to Cu^{2+} during the course of reaction.[6]

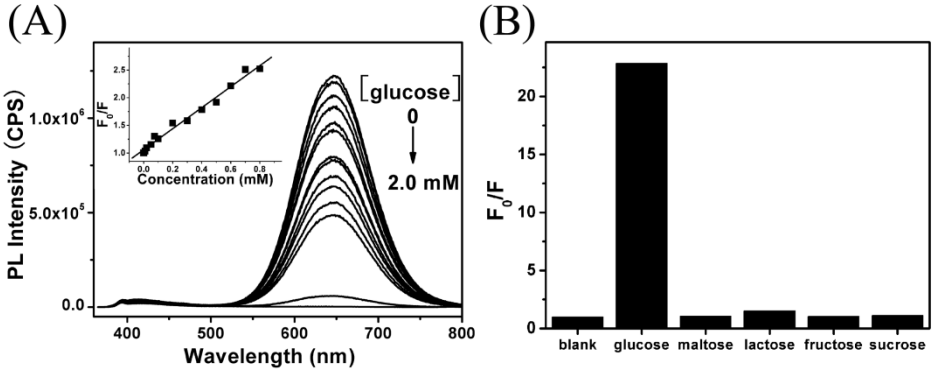

Fig. S16 (A) Effect of glucose concentration on the PL intensity of the CuNCs; inset: plots of F_0/F against the glucose concentration over the range 0~0.8 mM. (D) The selectivity of CuNCs for detection of glucose; the concentration of glucose and glucose analogues were 1 mM; F_0/F denotes the ratio of the PL intensities of the solutions in the absence and presence of glucose or glucose analogues.

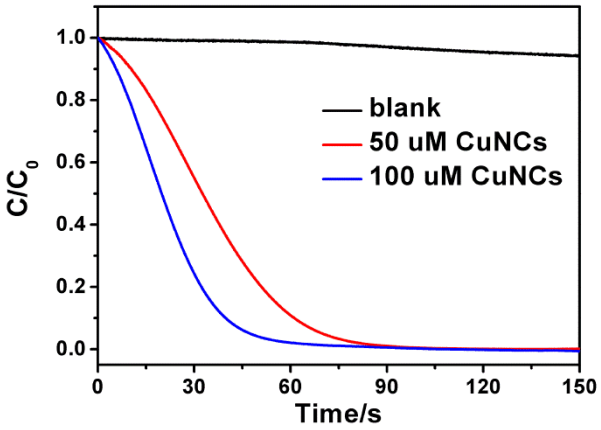

Fig. S17 C/C_0 versus reaction time for the reduction of MB as a function of time when 50 μM and 100 μM CuNCs were used, respectively.

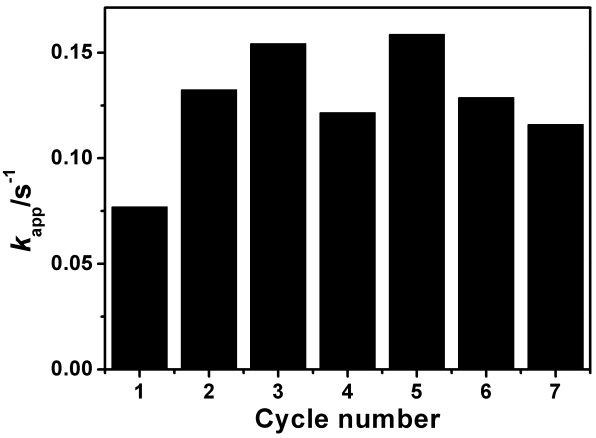

Fig. S18. Plots of observed reaction rate constant k_{app} against the number of successive catalytic MB reduction reactions.

To investigate the recyclability of the CuNCs, the CuNCs was subjected to recycling use. As show in the Fig. S18, the CuNCs retain their catalytic activity for 7 cycles. Because the

adsorption equilibrium between CuNCs and MB was not totally established initially, the catalytic activity at the first cycle was lower than that of the subsequent cycles.[1]

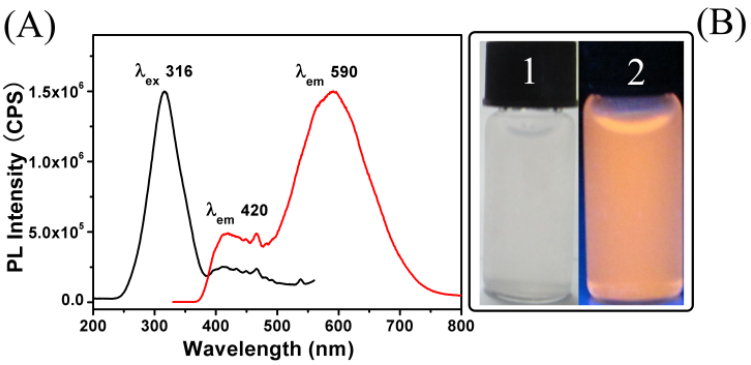

Fig. S19 (A) PL spectra of the as-prepared DPA-capped AgNCs; (B) Photographs of the as-prepared DPA-capped AgNCs under the irradiation of (1) visible and (2) UV light.

Upon excitation at 316 nm, two emission peaks at 420 nm and 590 nm were observed, with QY 4.1%. The PL lifetimes at 425 nm and 588 nm were determined to be 2.07 ns and 5.44 μs, respectively (Table S1). The obtained AgNCs is turbid but exhibits an orange color when irradiated with a UV lamp. As a complement to the well-studied AuNCs, this study provides a route to understand the general picture of luminescent metal NCs.

References

1. N. Vilar-Vidal, J. Rivas and M. Arturo Lopez-Quintela, *ACS Catal.*, 2012, **2**, 1693-1697.
2. J. Peisach and W. E. Blumberg, *Mol. Pharmacol.*, 1969, **5**, 200-209.
3. (a) H. Liu, Y. Ye, J. Chen, D. Lin, Z. Jiang, Z. Liu, B. Sun, L. Yang and J. Liu, *Chem. Eur. J.*, 2012, **18**, 8037-8041; (b) H. L. Hermann, G. Boche and P. Schwerdtfeger, *Chem. Eur. J.*, 2001, **7**, 5333-5342.
4. Z. Wu, E. Lanni, W. Chen, M. E. Bier, D. Ly and R. Jin, *J. Am. Chem. Soc.*, 2009, **131**, 16672-16674.
5. X. Jia, J. Li, L. Han, J. Ren, X. Yang and E. Wang, *ACS Nano*, 2012, **6**, 3311-3317.
6. K. J. Koski, J. J. Cha, B. W. Reed, C. D. Wessells, D. Kong and Y. Cui, *J. Am. Chem. Soc.*, 2012, **134**, 7584-7587.
7. D. Mott, J. Yin, M. Engelhard, R. Loukrakpam, P. Chang, G. Miller, I.-T. Bae, N. Chandra Das, C. Wang, J. Luo and C.-J. Zhong, *Chem. Mater.*, 2009, **22**, 261-271.